Clays and Clay Minerals, Vol. 53, No. 6, 564–571, 2005.

SORPTION AND DIRECT ELECTROCHEMISTRY OF MITOCHONDRIAL CYTOCHROME *C* ON HEMATITE SURFACES

NIDHI KHARE*, CARRICK M. EGGLESTON AND DAVID M. LOVELACE

Department of Geology and Geophysics, University of Wyoming, Laramie, Wyoming 82071, USA

Abstract—The interaction of cytochromes (heme proteins) with mineral surfaces is important from an environmental perspective (*e.g.* heavy metal remediation and reductive dehalogenation reactions), for designing biosensors and bioanalytical systems, and for emerging photovoltaic applications. In addition, the cytochrome studied here shares properties with some cytochromes from Fe-reducing bacteria and its general behavior sheds light on how other cytochromes might behave during Fe(III) reduction. The objectives of this study were to characterize the direct electrochemistry and sorption mechanism of horse heart ferricytochrome c (a mitochondrial cytochrome referred to as Hcc) on hematite surfaces as a function of pH, time of sorption and ionic strength. Hcc sorption on hematite mainly occurs between pH 8 and 10, the pH range in which hematite surfaces and Hcc are oppositely charged. Calculated net attractive forces correspond closely with the pH range of peak sorption, suggesting that sorption is mainly electrostatically controlled. Hcc sorption with ionic strength is consistent with this conclusion. The pH-dependent conformation of Hcc sorbed on hematite appears to be different from that in solution as indicated by UV-visible spectroscopy and its more negative reduction potential compared to native Hcc. Sorption kinetics were rapid and pH-independent across the pH range 3–10 with slow conformational changes occurring at >60 h. Our results suggest that the electrostatic attraction of the cytochrome towards the surface orient the cytochrome for favorable electron transfer between the heme group of the cytochrome and hematite.

Key Words—Cytochrome *c*, Fe Oxide, Hematite, Protein, Sorption.

INTRODUCTION

Cytochrome adsorption at the solid-liquid interface plays an important role in electron transfer, biosensor development, redox catalysis and bioremediation applications. For example, it has been shown that polyheme cytochromes with bihistidinyl Fe coordination can catalyze electron transfer to various oxides (Lojou *et al*., 1998). Reductive dehalogenation of halocarbon contaminants using cytochrome P-450 has been demonstrated (Castro *et al*., 1985; Shanker and Atkins, 1996; Wirtz *et al*., 2000). Protein-functionalized electrodes (Gorton *et al*., 1999; Kano and Ikeda, 2000; Fridman *et al*., 2000) have been used in sensor applications, including protein-functionalized Fe oxides (Cao *et al*., 2003). Recently, proteins and protein complexes have also been utilized in photovoltaic applications. Topoglidis *et al*. (2002) demonstrated a photovoltaic device using a nanocrystalline TiO_2 film photosensitized with the same protein we work with in this paper. Das *et al*. (2004) demonstrated a photovoltaic device made by immobilizing complete photosystem I (PSI) protein-cofactor complexes on modified indium-doped tin oxide (ITO). This device represents a remarkable integration of a biological photosystem into an oxide-based device.

Direct electron transfer between redox-active proteins (*e.g.* cytochromes) and electrodes is affected by sorption (Lojou and Bianco, 2000). Hence, characterizing sorption of cytochromes on mineral surfaces is useful for understanding electrochemical behavior essential to their application in biosensor and bioanalytical systems (Chen *et al*., 2002). For example, it has been shown that *c*-type cytochromes change conformation upon adsorption so as to affect electron transfer to mineral (kaolinite, montmorillonite, goethite) -modified electrode surfaces (Sallez *et al*., 2000). Slab optical wave guide spectroscopy (Santos *et al*., 2003), quartz microbalance techniques (Lojou and Bianco, 2003) and electrochemical surface-enhanced resonance Raman spectroscopy (Dick *et al*., 2000) have been used to study sorption and related conformation changes of cytochromes on surfaces. In addition, UV-visible spectroscopy was used *in situ* to indicate conformational alteration of myoglobin adsorbed on polymethylsiloxane (Anderson and Robertson, 1995). We elected to use wet chemical techniques (with UV-visible spectroscopy as a conformational probe) to characterize sorption of Hcc to hematite. Our objectives were (1) to characterize sorption of Hcc on hematite as a function of pH, time of sorption, and ionic strength; (2) to investigate the direct electrochemistry of Hcc on hematite; and (3) to monitor for possible conformation change using UV-visible spectroscopy and electrochemistry. Hematite was chosen because it is the only nominally ferric oxide that can be a sufficiently good semiconductor to use as an electrode in electrochemical experiments with cytochromes. Hcc has

* E-mail address of corresponding author:
Anidhi@uwyo.edu
DOI: 10.1346/CCMN.2005.0530602

been extensively studied and characterized, which provides us with as complete a comparative background for a cytochrome as exists; for example, conformational states and structural changes have been extensively correlated with UV-visible absorption bands, circular dichroism bands, and redox potentials so that changes in these properties can be readily interpreted in terms of protein folding. This degree of structural information is not available for most cytochromes (such as those utilized by dissimilatory Fe-reducing bacteria), and Hcc thus provides us with a very useful and indeed necessary first step in the characterization of other proteins interacting with oxide mineral surfaces.

EXPERIMENTAL METHODS

Hematite synthesis and characterization

Hematite was synthesized according to the method of Sugimoto *et al*. (1993), and powder X-ray diffraction (XRD) showed peaks characteristic of hematite. Synthesis yielded hematite platelets of ~1 μm diameter dominated by (001) surfaces as shown by scanning electron microscopy (SEM) images. The N_2 BET surface area of previous batches made using the same method was 4.76 m^2g^{-1}. Hematite was washed thrice with 1 M KCl solution and further washed with 0.01 M KCl to obtain a 0.01 M KCl background electrolyte (Khare *et al*., 2004) and stored as stock aqueous suspension of 94.1 g hematite kg^{-1} (measured) solids concentration.

Aqueous experiments

Sorption experiments for hematite suspensions were conducted in 30 mL polycarbonate centrifuge tubes following a procedure described by Khare *et al*. (2004). Protein retention to these tubes is minimal as per manufacturer's recommendation. All samples had a suspended solids concentration of 1.50 g kg^{-1}, constant ionic strength of 0.01 M KCl and total sample mass of 30±0.01 g. Aqueous solutions for sorption experiments (KCl, HCl, KOH all at 0.01 M and Hcc at 0.0001 M) were prepared using analytical-grade reagents and degassed (heated and N_2 purged) deionized water. Stock hematite suspension was shaken on a reciprocating shaker at 1 Hz for at least 30 min before use. 0.478 g of hematite was weighed while vigorously stirring a stock suspension on a magnetic stirrer, and brought to ~30% of the final mass with 0.01 M KCl. 5000 μL of 0.0001 M Hcc solution were added slowly to each vigorously stirred sample. The pH was adjusted using 0.01 M HCl or 0.01 M KOH, and each sample was brought to its final mass. The sample headspace was flushed with N_2 gas. To characterize the sorption kinetics, samples were shaken for 1, 5, 20, 40, 60, 90 and 120 h on a reciprocating floor shaker at 0.5 Hz and 21ºC. The pH varied by an average of 0.2 pH units and was not adjusted during equilibration. After equilibration, samples were centrifuged at ~6000 g for 10 min, and the supernatant solutions were decanted. The pH was measured in a portion of the supernatant solution before filtering and the remaining solutions were filtered using 0.2 μm polycarbonate filter membranes. Dissolved Hcc was measured in the supernatant solutions using UV-visible absorbance of the Soret band at 408 nm. The concentration of Hcc sorbed on hematite was determined as the difference between total added Hcc and Hcc measured in supernatant solutions.

To determinine the pH dependence of Hcc sorption, the pH was adjusted from 1.7 to 12.3. A 0.1 M HCl or 0.1 M KOH solution was used in addition to 0.01 M HCl or 0.01 M KOH to adjust the pH to 1.7, 2.0 or to 11.0, 12.0 or 12.3, respectively. To determine the ionic strength dependence of Hcc sorption, the background KCl concentration was varied from 0.1 to 0.5 M and the supernatant liquids were analyzed against standards of similar molarity. In addition, HCl and KOH of similar molarity were used for pH adjustment to achieve the desired ionic strength. For both the pH and ionic strength sorption dependence, the samples were equilibrated for 20 h and the pH was not adjusted during equilibration.

Model calculations

Hcc charge as a function of pH was calculated using an algorithm developed by Tabb (http://fields.scripps.edu/DTASelect/20010710-pI-Algorithm.pdf) that predicts the isoelectric point at pH 10, in agreement with Theorell and Akesson (1941). The surface charge of hematite as a function of pH was calculated using MICROQL and data from Stumm and Morgan (1996). As an approximation for van der Waals attraction, a Hamaker constant of 10^{-20} J was used with a simple block model (references in the caption of Figure 1b), giving an attractive force of ~0.05 nN. Hamaker constants for virus-hematite interaction through water (Vilker *et al*., 1981), if used as an approximation for protein-hematite interaction, give slightly smaller attractive forces. To estimate electrostatic forces between a hematite surface and Hcc, we used a point charge corresponding to the charge of an Hcc molecule positioned 1.0 nm above a 100 nm^2 area with a surface charge density calculated for the hematite surface using MICROQL. Hcc and hematite surface charge density for each pH were used in the pH-dependent force calculation; a dielectric constant of 10 was used as an approximation for interfacial structured water. Hexagonal close packing of 3.4 nm spheres (the size of Hcc in native globular conformation) was used to calculate the number of monolayers of Hcc sorbed on the surface of hematite. If Hcc unfolds and changes shape upon adsorption, however, this assumption may no longer apply. We offer the number of monolayers as one way of assessing the relative amount of adsorbed protein; it should be thought of as a monolayer equivalent for hexagonally close-packed native globular protein based simply on the amount of available surface area and the amount of sorbed protein.

Conformation of Hcc using UV-visible spectroscopy

The absorbance of heme proteins in the visible region (*i.e.* the Soret band) depends directly on the physical environment of the heme (Anderson and Robertson, 1995). The Soret band of Hcc in solution thus gives an indication of its conformational state (*e.g.* as a function of pH), but are not necessarily structurally specific; conformational changes ranging from relaxation of the heme pocket to a complete disruption of secondary and tertiary structure could account for the altered heme environment (Anderson and Robertson, 1995).

Electrochemical characterization of Hcc using hematite electrodes

Cyclic voltammograms (CV) were obtained using a hematite (single crystal) working electrode, Pt wire counter electrode and an oxidized Ag wire pseudo-reference calibrated against an Ag/AgCl reference electrode. Clean hematite crystals with electron donor impurity (Sn and Ti) concentration of 2×10^{-3} atom.% were suspended in 0.1 M KCl with or without added Hcc. The CVs were collected using a EG&G 263 A potentiostat controlled using a PC.

RESULTS AND DISCUSSION

Conformation and Hcc sorption on hematite as a function of pH

Hcc sorption isotherms at pH 4, 6.8 and 9.5 are shown in Figure 1a. Sorption was minimal at pH 4, increased slightly at pH 6.8, and showed a pronounced increase at pH 9.5 (Figure 1a). These isotherms differ from those of other proteins (human plasma albumin, HPA, and bovine pancreas ribonuclease, Rnase) sorbing to hematite in that they do not show well expressed plateau values (Koutsoukos *et al*., 1983). Our adsorption envelope results showed that Hcc sorption depended strongly on pH, with most sorption occurring between pH 8 and 10 (Figure 1b). The isoelectric point of Hcc is ~10 (*e.g.* Theorell and Akesson, 1941) while the point of zero charge for hematite is ~pH 8.5 (*e.g.* Parks and deBruyn, 1962); hence, the narrow pH range of sorption (at pH values for which we would expect opposite charge on the Hcc and hematite) suggests a primarily electrostatic attraction. We estimated electrostatic and van der Waals forces (see Methods) between hematite and Hcc, and the resulting pH-dependent net forces are plotted in Figure 1b. The peak in Hcc sorption coincides well with the calculated region of net attractive force (Figure 1b).

Hcc is a folded protein that changes conformation with pH (Boffi *et al*., 2001), affecting optical absorption. At pH<3.0, intramolecular electrostatic repulsion leads to unfolding and the exposure of hydrophobic portions of the molecule to solution (which may affect adsorption) and is reflected in a blue shift in the Soret band position (Figure 2a). In the pH 3–7 range there is no shift in Soret band position, but from pH 7 to 12 there is a small

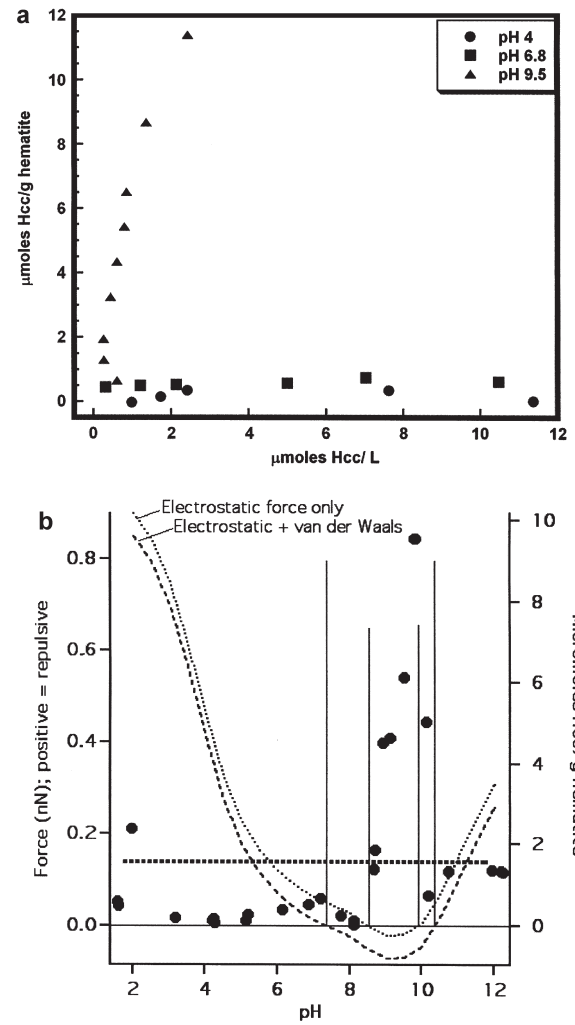

Figure 1. (a) Sorption isotherms of µmoles of Hcc sorbed/g of hematite *vs.* µmoles of dissolved Hcc/L of supernatant solution at pH 4.0±0.05, 6.83±0.07, and 9.5±0.10. (b) Sorption of Hcc on hematite as a function of pH (filled circles, right-hand axis). Black dotted and dashed curves give overall repulsive (positive) or attractive (negative) forces between hematite and Hcc (references for Hcc isoelectric point and hematite point of zero charge are given in the text; Hamaker constant for van der Waals calculation from Schudel *et al*. (1997) and Neal *et al*. (1999)). The thick dashed horizontal line gives the amount of sorption corresponding to one monolayer of Hcc on hematite in hexagonal close packing. The vertical lines show the zero crossing points for the force calculations with and without van der Waals forces for easier comparison to the sorption data.

but systematic blue shift of 3 nm (Figure 2a). Thus, there may be conformational changes taking place in the pH range of peak adsorption (pH 8 to 10) that could affect the adsorption reaction. Nevertheless, the clear correspondence between peak adsorption and electrostatic attraction (Figure 1b) suggests that possible conformational changes (for example) in the hydrophobic *vs*. hydrophilic nature of Hcc are not contributing in an obvious way to adsorption.

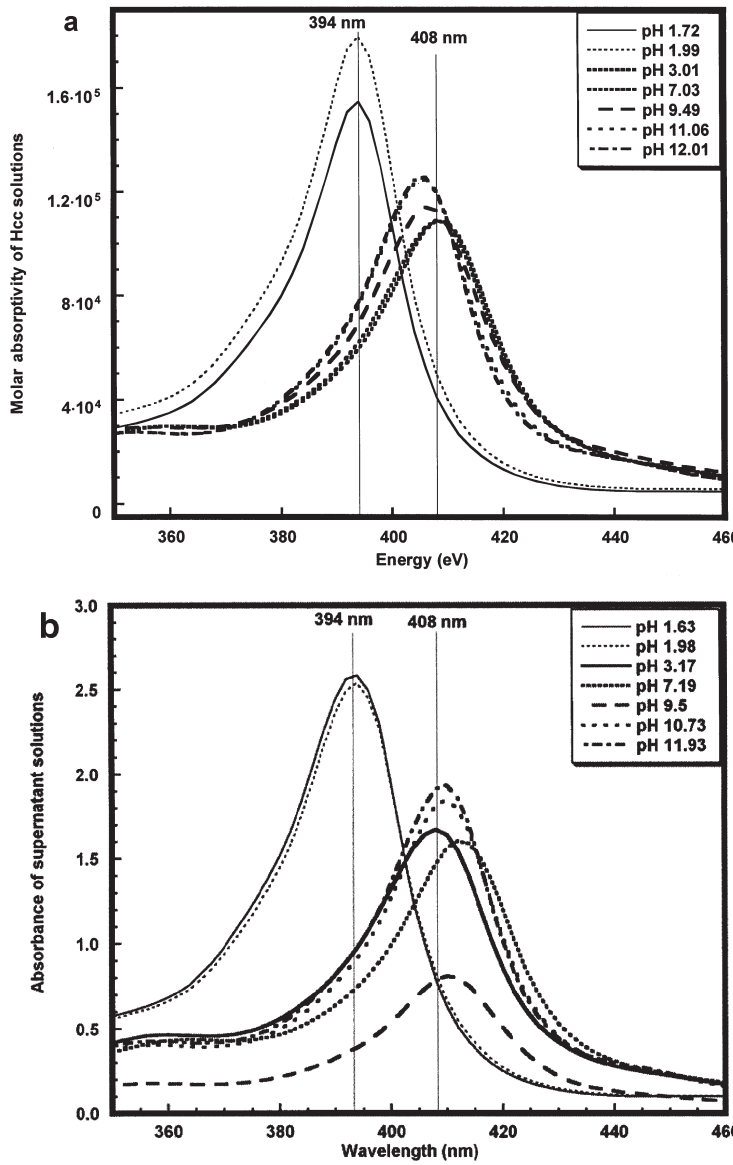

Figure 2. UV-visible absorption spectra showing the Soret band as a function of pH; (a) molar absorptivity of Hcc solutions; (b) absorbance of supernatant solutions of Hcc sorbed on hematite. Because the concentration of Hcc in the supernatant solutions was based on molar absorptivity in solutions, the molar absorptivity of the supernatant solutions could not be compared independently.

Following Hcc sorption experiments, background electrolyte was added; we found negligible desorption, indicating that sorption was irreversible with dilution (similar to Koutsoukos *et al*., 1983). However, 80–100% desorption occurred upon changing the pH to 4 (data not shown). This result provides additional evidence for electrostatic binding, because a change in pH changes the electrostatic interaction between hematite and Hcc, whereas dilution at constant pH does not.

Adsorption of Hcc on quartz and other mineral oxide surfaces has previously been attributed mainly to electrostatic interactions (Santos *et al*., 2003; Sallez *et al*., 2000). The operation of Hcc in its physiological setting (interaction with biological membranes and with cytochrome *c* oxidase) is thought to be primarily electrostatically controlled (*e.g.* Pinheiro 1994; Millett and Durham, 1996). Pinheiro (1994) showed that two different conformational states are induced in Hcc upon complexation with negatively charged surfaces. The conformation of state I is similar to that of Hcc in solution where native low-spin Fe configuration of heme is preserved, but in state II the heme groove opens leading to thermal and potential dependent equilibrium between a 5-coordinated high-spin and a 6-coordinated low-spin configuration. The equilibrium between states I and II as well as the conformation equilibrium in state II appear to be controlled by the electrostatic interaction between the positively charged lysine residues surround-

ing the heme groove and a negatively charged surface (Pinheiro 1994), similar to the situation expected for adsorption to hematite at pH >pzc.

Conformational changes upon sorption that might affect the ability of Hcc to desorb, and hence also its overall sorption behavior needs to be considered. Our Hcc supernatant solutions, in the context of microscopic reversibility, can be considered to be a mixture of 'native' Hcc that has never been sorbed to hematite with Hcc that has been sorbed and then desorbed. The UV-visible spectra for supernatant solutions at pH 7–12 were red-shifted, while those for Hcc solutions in the same range showed a systematic blue shift (Figure 2a,b). These differences suggest a conformational change, caused by sorption, that is carried into solution upon subsequent desorption. This in turn suggests that 20 h of reaction time is insufficient to equilibrate with respect to a slow exchange process between surface and solution.

The peak sorption occurs with a surface coverage equal to ~7 monolayers of Hcc (Figure 1b). This high surface coverage is probably caused by a combination of factors, including (1) van der Waals attraction between Hcc molecules near the Hcc isoelectric point, leading to agglomeration, (2) alignment of the Hcc dipoles negative-to-positive as a result of orientation in the weak electric field between pH 8.5 and 10, and (3) possible conformational change of Hcc in the sorbed state such that the assumption of 3.4 nm spheres used to calculate monolayer coverage no longer holds.

Kinetics of Hcc sorption on hematite

The rate of initial sorption was rapid and essentially constant over the pH range, 3–10 with Hcc reaching 85–90% of its maximum sorption capacity within an hour (Figure 3a). Sorption kinetics and amounts appear similar at pH 3 and 7 (Figure 3a). At pH 9.7, after ~60 h, the total amount of sorbed Hcc appears to decrease slowly. Because the amount of sorption is extremely sensitive to pH in this range (Figure 2a), differences in pH as shown in the error bars could result in apparent reduction in sorption. In addition, the blue shift in the position of the Soret band with time (at pH 9.66; Figure 3b) suggests that Hcc of altered conformation might be slowly building up in solution. As indicated in the UV-visible results, such shifts can also result in higher optical absorptivities than native protein (which could cause an artifactual apparent decrease in sorption). Hence, because longer-term variations in apparent sorption density may be related to slow conformation change rather than to absolute amounts of adsorption, an operational equilibration time of 20 h for pH and ionic strength-dependent experiments was chosen.

Hcc sorption on hematite as a function of ionic strength

At pH 3.0 and 6.7, below the IEP of both hematite and Hcc, repulsive net electrostatic forces exist between hematite and Hcc, and there is very little sorption (Figure 4a). Ionic strength has little effect on the amount of Hcc sorbed, which hovers within error of zero (Figure 4a). At pH 9.5, between the IEP of hematite and Hcc, there is electrostatic attraction between hematite and Hcc; if Hcc is treated as a diffuse layer ion attracted to the vicinity of a charged surface, we would expect to see the total amount sorbed to decrease with ionic strength at pH 9.5. This seems to be the case, with the exception of sorption at 300 mM KCl. At pH 9.5, there is a relatively high molar absorptivity at 100 mM KCl, but a relatively low molar absorptivity at 300 mM KCl; this appears to correlate inversely with the adsorption results at these KCl concentrations (Figure 4b). In contrast, there is essentially no variability for the results at pH 3.0 (Figure 4b). We emphasize that we have calibrated the concentration measurement at each ionic strength value, so that an unusually small molar absorptivity at 300 mM does not lead to an artificially low concentration measurement at 300 mM and thus to an artificially high sorption density for Hcc. Instead, the changes in molar absorptivity may reflect conformation changes in the Hcc that affect its ability to sorb. In addition, the full width at half

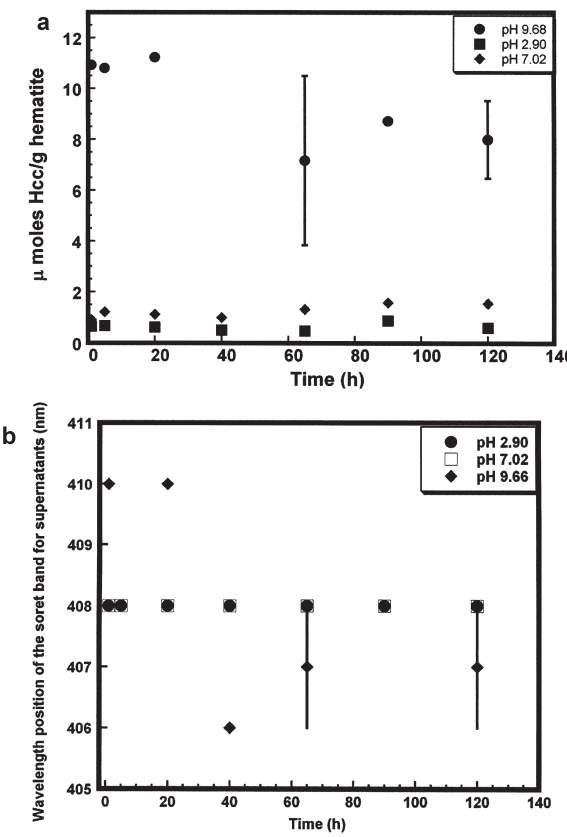

Figure 3. (a) Sorption kinetics for Hcc sorbing on hematite over a period of 1–120 h for pH 2.9, 7.0 and 9.7; (b) wavelength position of Soret bands in supernatant solutions from sorption experiments as a function of time at pH 2.9, 7.0 and 9.7.

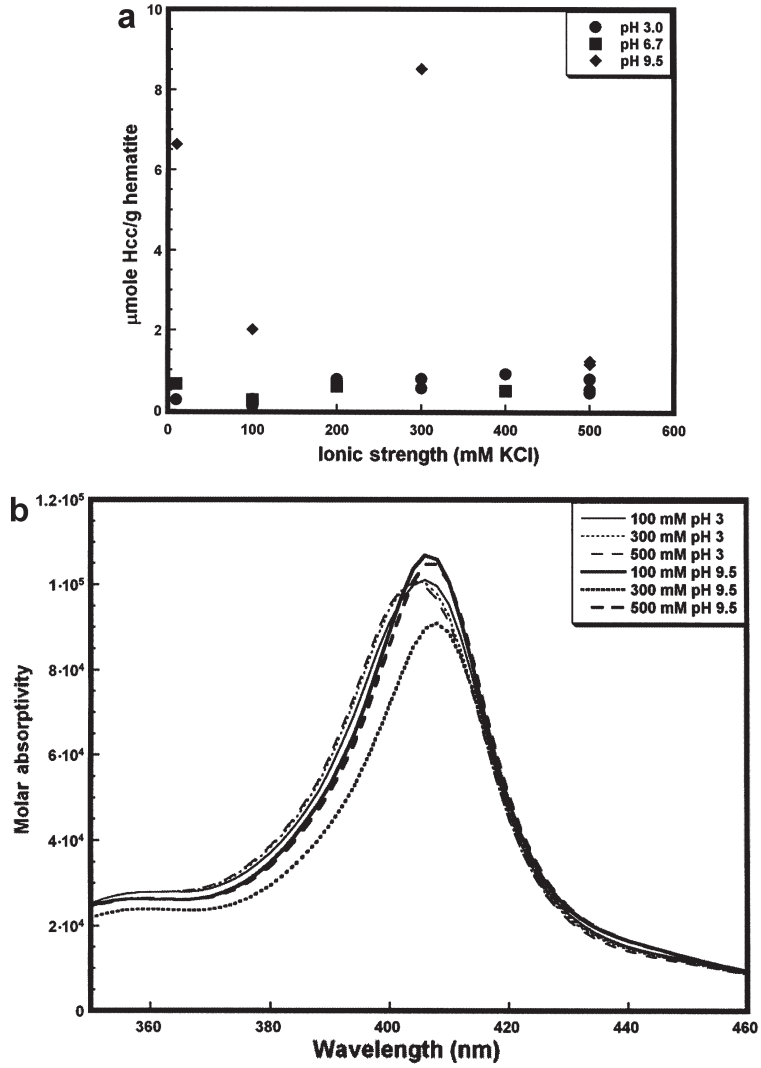

Figure 4. (a) Ionic strength dependence of Hcc sorption on hematite at pH 3.0, 6.7 and 9.5; (b) UV-visible spectra for Hcc in solution at pH 3.0 and 9.5 at 100, 300 and 500 mM background electrolyte (KCl) concentration showing changes in molar absorptivity with ionic strength at pH 9.5.

maximum height (fwhm) for the Soret band in our absorption spectra does not increase with increasing ionic strength, suggesting that Hcc aggregation did not occur in our systems (Whitford *et al*., 1991; Peng *et al*., 2000).

Direct electrochemistry of Hcc on hematite

Direct electrochemistry of Hcc on hematite was demonstrated (Figure 5). In later scans, a reduction wave at positive potential grows into the voltammograms and the oxidation broadens on the high-potential side. The average of the initial reduction and oxidation wave potentials gives a measured midpoint potential of ~10 mV positive (relative to the Ag/AgCl reference), which is slightly below that expected for native Hcc at 50 mV (Yeh and Kuwana, 1977; Bowden *et al*., 1984; Chen *et al*., 2002). The higher-potential waves have been observed previously and attributed to hemes experiencing a positive charge environment (Chen *et al*., 2002). The slightly negative reduction potential compared to native cytochromes suggest that at pH 9.5 slight unfolding of Hcc may have taken place due to sorption on hematite consistent with the results from UV-visible spectroscopy. Voltammograms taken without Hcc (control) show no peaks (data not shown).

CONCLUSIONS

Sorption of Hcc to hematite is dominated by electrostatic attraction that should orient Hcc molecules with the heme (redox center) relatively close to the hematite surface, consistent with successful direct electrochemistry of Hcc using hematite electrodes. Sorption is probably a preliminary step before electron

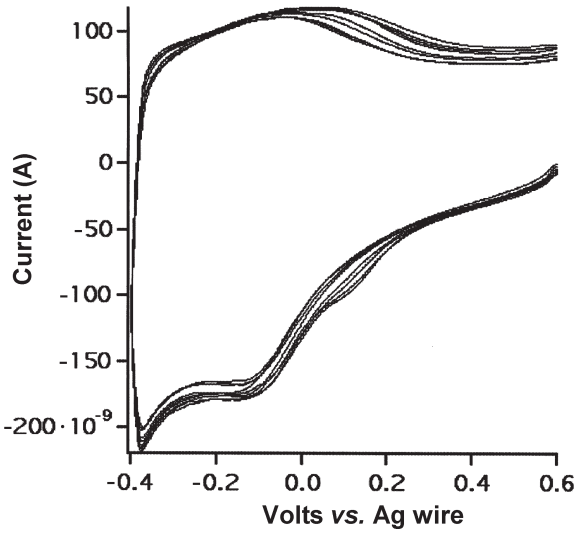

Figure 5. Cyclic voltammograms (current *vs*. potential) of Hcc solution at pH 9.5 using a hematite working electrode, Pt wire counter electrode and an Ag wire pseudo-reference calibrated to an Ag/AgCl reference electrode.

transfer between hematite surfaces and cytochromes. We have no direct evidence of major conformation change upon sorption, but the unusually high sorption density, red-shifts in Soret band absorption of supernatant solutions, and a slightly negative reduction potential are possible indirect evidence of conformation change induced by adsorption. The ionic strength dependence of Hcc sorption is consistent with mainly electrostatic binding. In addition, van der Waals attractive forces probably contribute to sorption. Hcc sorption is initially quite rapid, but at pH 9.6 the apparent amount sorbed decreases for times greater than 60 h; this decrease may be related to slow conformation change.

REFERENCES

Anderson, A.B., and Robertson, C.R. (1995) Absorption spectra indicate conformational alteration of myoglobin adsorbed on polymethylsiloxane. *Biophysical Journal*, **68**, 2091–2097.

Boffi, F., Bonincontro, S., Cinelli, A., Castellano, C., Francesco, A. De, Della Longa, S., Girasole, M. and Onori, G (2001) pH dependent local structure of ferricytochrome c studied by X-ray absorption spectroscopy. *Biophysical Journal*, **80**, 1473–1479.

Bowden, E.F., Hawkridge, F.M. and Blount, H.N. (1984) Interfacial electrochemistry of cytochrome c at tin oxide, indium oxide, gold, and platinum electrodes. *Journal of Electroanalytical Chemistry*, **161**, 355–376.

Cao, D., He, P. and Hu, N. (2003) Electrochemical biosensors utilizing electron transfer in heme proteins immobilized on Fe_3O_4 nanoparticles. *Analyst*, **128**, 1268–1274.

Castro, C.E., Wade, R.S. and Belser, N.O. (1985) Biodehalogenation: Reactions of cytochrome P-450 with polyhalomethanes. *Biochemistry*, **24**, 204–210.

Chen, X., Ferrigno, R., Yang, J. and Whitesides, G.M. (2002) Redox properties of cytochrome c adsorbed on self-assembled monolayers: A probe for protein conformation and orientation. *Langmuir*, **18**, 7009–7015.

Das, R., Kiley, P.J., Segal, M., Norville, J., Yu, A.A., Wang, L., Trammell, S.A., Reddick, L.E., Kumar, R., Stellacci, F., Lebedev, N., Schnur, J., Bruce, B.D., Zhang S. and Baldo, M. (2004) Integration of photosynthetic protein molecular complexes in solid-state electronic devices. *Nano Letters*, **4**, 1079–1083.

Dick, L.A., Haes, A.J. and Van Duyne, R.P. (2000) Distance and orientation dependence of heterogeneous electron transfer: A surface-enhanced resonance Raman scattering study of cytochrome c bound to carboxylic acid terminated alkanethiols adsorbed on silver electrodes. *Journal of Physical Chemistry*, **104**, 11752–11762.

Fridman, V., Wollenberger, U., Bogdanovskaya, V., Lisdat, F., Ruzgas, T., Lindgren, A., Gorton, L. and Scheller, F.W. (2000) Biosensors and novel bioanalytical methods. *Biochemical Society Transactions*, **28(2)**, 63–70.

Gorton, L., Lindgren, A., Larsson, T., Munteanu, F.D., Ruzzas, T. and Gazaryan, I. (1999) Direct electron transfer between heme containing enzymes and electrodes as basis for third generation biosensors. *Analytica Chimica Acta*, **400(103)**, 91–108.

Kano, K. and Ikeda, T. (2000) Fundamentals and practices of mediated bioelectrocatalysis. *Analytical Sciences*, **16(10)**, 1013–1021.

Khare, N., Hesterberg, D., Beauchemin, S. and Wang, S.-L. (2004) XANES determination of adsorbed phosphate distribution between ferrihydrite and boehmite in mixtures. *Soil Science Society of America Journal*, **68**, 460–469.

Koutsoukos, P.G., Norde, W. and Lyklema, J. (1983) Protein adsorption on hematite (α-Fe_2O_3) surfaces. *Journal of Colloid and Interface Science*, **95**, 385–396.

Lojou, E. and Bianco, P. (2000) Membrane electrodes can modulate the electrochemical response of redox proteins – direct electrochemistry of cytochrome c. *Journal of Electroanalytical Chemistry*, **485**, 71–80.

Lojou, E. and Bianco, P. (2003) Quartz crystal microbalance and voltammetry monitoring for layer by layer assembly of cytochrome c3 and poly (ester sulfonic acid) films on gold and silver electrodes. *Journal of Electroanalytical Chemistry*, **557**, 37–47.

Lojou, E., Bianco, P. and Bruschi, M. (1998) Kinetic studies on the electron transfer between bacterial c-type cytochromes and metal oxides. *Journal of Electroanalytical Chemistry*, **452**, 167–177.

Millett, F. and Durham, B. (1996) Chemical modification of surface residues on cytochrome c. Pp. 573–591 in: Cytochrome-c: A multidisciplinary Approach (R.A. Scott and A. Grant Mauk, editors). University Science Books, Sausalito, California.

Neal, B.L., Asthagiri, D., Velev, O.D., Lenhoff, A.M. and Kaler, E.W. (1999) Why is the osmotic second virial coefficient related to protein crystallization? *Journal of Crystal Growth*, **196**, 377–387.

Parks, G.A. and De Bruyn, P.L. (1962) The zero point of charge of oxides. *Journal of Physical Chemistry*, **66**, 967–973.

Peng, X., Huang, J. and Ji, L. (2000) The self aggregation of Chiral threonine-linked porphyrins and their Zn(II) complexes. *Chinese Science Bulletin*, **45**, 418–421.

Pinheiro, T.J.T. (1994) The interaction of horse heart cytochrome c with phospholipid bilayers. Structural and dynamic effects. *Biochimie*, **76**, 489–500.

Sallez, Y., Bianco, P. and Lojou, E. (2000) Electrochemical behavior of c-type cytochromes at clay-modified carbon electrodes: A model for the interaction between proteins and soils. *Journal of Electroanalytical Chemistry*, **493**, 37–49.

Santos, J.H., Matsuda, N., Qi, Z.-M., Yoshida, T., Takatsu, A. and Kato, K. (2003) Adsorption behavior of cytochrome c,

myoglobin and haemoglobin in a quartz surface probed using slab optical waveguide (SOWG) spectroscopy. *Analytical Sciences*, **19**, 199–204.

Schudel, M., Behrens, S.H., Holthoff, H., Kretzschmar, R. and Borkovec, M. (1997) Absolute aggregation rate constants of hematite particles in aqueous suspensions: A comparison of two different surface morphologies. *Journal of Colloid and Interface Science*, **196**, 241–253.

Shanker, R. and Atkins, W.M. (1996) Luciferase-dependent, cytochrome P-450-catalyzed dehalogenation in genetically engineered *Pseudomonas*. *Biotechnology Progress*, **12**, 474–479.

Sugimoto, T., Muramatsu, A., Sakata, K. and Shindo, D. (1993) Characterization of hematite particles of different shapes. *Journal of Colloid and Interface Science*, **158**, 420–428.

Stumm, W. and Morgan, J.J. (1996) *Aquatic Chemistry*, 3rd edition. John Wiley & Sons, Inc., New York.

Theorell, H. and Akesson, A. (1941) Studies on cytochrome c. III. Titration curves. *Journal of the American Chemical Society*, **63**, 1818–1820.

Topoglidis, E., Campbell, C.J., Palomares, E. and Durrant, J.R. (2002) Photoelectrochemical study of Zn cytochrome-c immobilized on a nanoporous metal oxide electrode. *Chemical Communications*, **2002**, 1518–1519.

Vilker, V.L., Uyeno, G.P. and McMillan, W.G. (1981) Solvent effect on the dispersion (Hamaker-London) coefficient from third-order perturbation theory. *Journal of Physical Chemistry*, **85**, 2013–2021.

Whitford, D., Concar, D.W. and Williams, R.J.P. (1991) The promotion of self-association of horse-heart cytochrome c by hexametaphosphate anions. *European Journal of Biochemistry*, **199**, 561–568.

Wirtz, M., Klucik, J. and Rivera, M. (2000) Ferredoxin mediated electrocatalytic dehalogenation of haloalkanes by cytochrome $P450_{cam}$. *Journal of the American Chemical Society*, **122(6)**, 1047–1056.

Yeh, P. and Kuwana, T. (1977) Reversible electrode reaction of cytochrome c. *Chemistry Letters*, **1977**, 1145–1148.

(*Received 17 September 2004; revised 16 May 2005; Ms. 961; A.E. Hailiang Dong*)